Transmembrane Ion Channels Constructed of Cholic Acid Derivatives

Yoshiaki Kobuke*,† and Takeshi Nagatani§

Graduate School of Materials Science, Nara Institute of Science and Technology, and CREST, Japan Science and Technology Corporation (JST), 8916-5 Takayama, Ikoma, 630-0101, Japan, and Department of Materials Science, Faculty of Engineering, Shizuoka University, 3-5-1, Johoku, Hamamatsu 432-8011, Japan

kobuke@ms.aist-nara.ac.jp

Received February 26, 2001

A new class of supramolecular transmembrane ion channels was prepared by linking two amphiphilic cholic acid methyl ethers through biscarbamate bonds to afford bis(7,12-dimethyl-24-carboxy-3-cholanyl)-*N*,*N*′-xylylene dicarbamate **2** and bis[7,12-dimethyl-24-(*N*,*N*,*N*-trimethylethanaminium-2-carboxylate)-3-cholanyl]-*N*,*N*′-xylylene dicarbamate dichloride **3**. When incorporated into a planar bilayer membrane, both compounds showed stable (lasting 10 ms to10 s) single ion channel currents. Only limited numbers of relatively small conductances were characterized for these channels (5−20 pS for **2** and 5−10 pS for **3**, 10 and 17 pS for **2**, and 9 pS for **3** in particular). Both channels were cation selective, and permeability ratios of potassium cation to chloride anion were 17 and 7.9 for **2** and **3**, respectively, reflecting the difference in ionic species of the headgroup. Both channels **2** and **3** showed significant potassium selectivity over sodium by a factor of 3.1 and 3.2, respectively. No Li^+ currents were observed for **2**, showing sharp discrimination between Na^+ or K^+.

Introduction

Stimuli received at sensory organs distributed in the animal body are converted to electrical signals in various ways and transmitted up to the central nervous system. The signal is treated appropriately there, and the responding order is conveyed back to terminal organs to commence actions. In these processes, electrical signals are transferred along the nerve axon in the form of nonattenuating waves of membrane potentials. In all facets of these events involving the generation and conduction of electrical signals, ion channels play the most important role in producing ionic fluxes across biological membranes.[1] Mimics of this biologically important function are interesting from various aspects underlying science and technology. Real understanding of the scientific principle underlying expression of these functions in nature may best be tested and deepened by constructing molecules of functional components. Another viewpoint is the application of these excellent functions in molecular ionics devices, sensory amplification systems, and other applications. In both cases, it is important that even sophisticated functions should be expressed by the most simple principles and molecules as possible.

In 1992, we succeeded in observing single-channel currents by incorporating an ion pair of oligo(oxybutylene)carboxylate with dialkylammonium into bilayer lipid membranes.[2] Despite its simple structural unit, the observed current behavior was almost identical with those of natural ion channels. In other words, a constant current was observed upon application of a membrane voltage, the system displaying an ohmic relationship between current (I) and voltage (V) values as well as frequent open-closed transitions. The conductances obtained from $I-V$ plots of repeated runs varied in the range 10^0-10^3 pS. Such behavior was accounted for by assuming supramolecular ion channel formation by connection of two-half-channel units across the bilayer membranes. After this observation we attempted to introduce several novel functions into ion channels and succeeded in obtaining voltage gating and photocontrol of ionic fluxes by using half channels not only of molecular assemblies,[3] but of a unimolecular source.[4] Various other approaches have been reported by other resaerch groups.[5]

Most recently, we introduced a simple cholic acid derivative **1** for observing stable single-channel currents.[6] A rigid and hydrophobic steroidal skeleton and three methoxyl substituents extruded into its concave space afforded ideal molecular amphiphilicity to provide the structural component of supramolecular ion channel. This unit served as one of the simplest expressions of an artificial ion channel to give single-channel currents with long-lasting stable open states.

To take the research a step further, it is necessary to develop a fundamental structural unit to create membrane penetrating ion channels in order to attempt more sophisticated control of ionic flux across membranes.

* Address correspondence to this author.
† Nara Institute of Science and Technology and CREST.
§ Shizuoka University.

(1) Hille, B. *Ionic Channels of Excitable Membranes*, 2nd ed.; Sinauer: Sunderland, MA, 1992.
(2) Kobuke, Y.; Ueda, K.; Sokabe, M. *J. Am. Chem. Soc.* **1992**, *114*, 7618−7622.
(3) (a) Kobuke, Y.; Ueda, K.; Sokabe, M. *Chem. Lett.* **1995**, 435−436. (b) Kobuke, Y.; Morita, K. *Inorg. Chim. Acta* **1998**, *283*, 167−174. (c) Kobuke, Y.; Ohgoshi, A. *Colloids Surf., A: Physicochem. Eng. Aspects* **2000**, *169*, 187−197.
(4) Tanaka, Y.; Kobuke, Y.; Sokabe, M. *Angew. Chem., Int. Ed. Engl.* **1995**, *34*, 693−694.

10.1021/jo010208i CCC: $20.00
Published on Web 07/04/2001

Here, we have designed molecules by connecting two cholic acid methyl ether derivatives to obtain a membrane-penetrating component creating supramolecular ion channels. Basic properties of these artificial ion channels are characterized via measurement of single ion-channel currents.

Results

Synthesis of Transmembrane Ion Channels. Carboxylate or ammonium headgroups were attached to terminals of methylcholic acid derivatives by bisurethane linking in the hope that carboxyl and ammonium groups may modulate charge and metal ion selectivities at the entrance of the transmembrane channels. The synthetic route to ion channel units **2** and **3** is outlined in Scheme 1. Selective protection of the 3-hydroxyl group of methyl cholate was undertaken by using a slight excess of dihydropyrane while cooling in ice. Since this hydroxyl group is known to be the most reactive, the other two hydroxyl groups, which remained unaffected, were then permethylated, and deprotection of 3-itetrahydropyranyl ether gave rise to the formation of **6** with a free 3-hydroxyl group. Two components of **6** were connected by bisurethane linkages by the reaction with xylylene diisocyanate in the presence of diazabicylo[2.2.2]octane in a yield of 45%. Diester **7** was then converted to diacid **2** as one of the target compounds. The ester functionalities of **7** were reduced selectively with lithium borohydride to hydroxymethyl groups, which were then esterified by betain acid chloride in order to introduce trimethylammonium terminals on to both molecular ends. ^{1}H NMR spectra of these membrane-spanning compounds **2** and **3** exhibited characteristic peaks due to benzylic protons and (3-)CH−O−CO protons appeared at 4.38 and 4.47 ppm for **2** and 4.32 and 4.49 ppm for **3**, respectively. The integral ratios of OCH_3/$BzCH_2N$/CHOCO peaks corresponded quite closely to the calculated 6:4:2 for both of compounds. Aromatic protons of the central linking part were obscured by overlap with the solvent peak in $CHCl_3$ but were confirmed by measurement of the spectrum in DMSO-d_6. The mass spectrum of **2** gave M + Na^+ and M + K^+ peaks at 1083.94 (calcd 1083.69) and 1099.98 (calcd 1099.66), respectively, and confirmed the desired coupling structure. In the case of **3**, the integral ratio of the trimethylammonium peak at 3.65 ppm corresponded to 9H relative to the other peaks, and the ESI mass spectrum gave a peak at 616.3 *m*/*z* corresponding to the double cationic species M^{2+} (calcd 616.455). The correct mass number and the symmetrical NMR spectrum confirmed the successful introduction of two betainic acid units in both of the terminal positions. Finally, both of compounds gave CH analyses in agreement with the expected structure.

Single-Channel Conductance and Open-Closed Transition Behavior. When 0.1−5 wt % of **2** relative to the lipid was incorporated into a planar bilayer membrane, stable single ion channel currents were observed. Most experiments employed 1 wt % of **2**. A typical record is illustrated in Figure 1a under the symmetric salt conditions of $[KCl]_{cis} = [KCl]_{trans} = 500$ mM, pH = 7.2 (HEPES/Tris) at a membrane voltage of +73 mV. The open and closed durations are clearly long compared to those of supramolecular or unimolecular half channels containing a simple alkyl chain as the membrane-inserting unit. The dwell time in the open state was determined to be on the order of 10^{-2}−10^{1} s, the most probable time being in the order 10^{-1} to 10^{0} s. Similar behavior has recently been observed for the supramolecular ion channel constructed from steroidal half channel units,[6] but the open lifetimes observed here are clearly longer. The histogram analysis of the current for the whole period at this voltage gave a value of 0.53 pA (Figure 1b). Upon variation of the membrane voltages, the currents observed were plotted against the voltage to give a linear relationship as shown in Figure 1c, from which the conductance was determined as 17 pS for this run. These measurements were repeated several times, incorporating independent samples and using a membrane spanning into the orifice separating two cell chambers. A histogram of all the observed conductances is illustrated in Figure 2. Two main conductance levels at 10 and 17 pS were observed for **2**.

In the case of **3**, similar characteristics were observed for the open-closed times which showed a relatively long open time in the region 10 ms to 10 s, particularly concentrating in the region 100 ms to 1 s. The conductances also appeared to be similar, but in a slightly smaller range of 5−10 pS, particularly concentrating in the region around 9 pS under the same bath solution conditions.

Charge Selectivity. The current−voltage plots under asymmetric conditions, $[KCl]_{cis} = 500$mM, $[KCl]_{trans} = 100$mM, pH = 7.2 were obtained for **2** and **3** (Figures 1 and 2 of the Supporting Information). From the plot, reversal potentials E_{rev}'s were estimated and put into the Goldman−Hodgkin−Katz equation to obtain the permeability selectivity ratio P_{K^+}/P_{Cl^-}. Similar experiments were undertaken using KBr, and the following equations summarize the permeability selectivity ratios of cation to anion:

$$\mathbf{2}: \; P_{K^+}/P_{Cl^-} = 17, \; P_{K^+}/P_{Br^-} = 5.6$$

$$\mathbf{3}: \; P_{K^+}/P_{Cl^-} = 7.9, \; P_{K^+}/P_{Br^-} = 4.4$$

(5) Reviews: (a) Kobuke, Y. In *Towards Molecular Biophysics of Ion Channels, Progress in Cell Research*; Sokabe, M., Auerbach, A., Sigworth, F., Ed.; Elsevier: Amsterdam, 1997; Vol. 6, pp 167−188. (b) Kobuke, Y. In *Advances in Supramolecular Chemistry*; Gokel, G. W., Ed.; JAI Press: London, 1998; Vol. 4, pp 163−209. (c) Gokel, G. W.; Murillo, O. *Acc. Chem. Res.* **1996**, *29*, 425−432. (d) Fyles, T. M.; van Straaten-Nijenhuis, W. F. In *Comprehensive Supramolecular Chemistry*; Reinhoudt, D. N. Ed.; Elsevier Science Ltd.: Oxford, 1996; pp 53−77. (e) Voyer, N. *Top. Curr. Chem.* **1996**, *184*, 1−37. More recent artificial ion channels have been reported; see: (f) Lear, J. D.; Schneider, J. P.; Kienker, P. K.; DeGrado, W. F. *J. Am. Chem. Soc.* **1997**, *119*, 3212−3217. (g) Dieckmann, G. R.; Lear, J. D.; Zhong, Q.; Klein, M. L.; DeGrado, W. F.; Sharp, K. A. *Biophys. J.* **1999**, *76*, 618−630. (h) Fyles, T. M.; Loock, D.; Zhou, X. *J. Am. Chem. Soc.* **1998**, *120*, 2997−3003. (i) Clark, T. D.; Buehler, L. K.; Ghadiri, M. R. *J. Am. Chem. Soc.* **1998**, *120*, 651−656. (j) Schrey, A.; Vescovi, A,; Knoll, A.; Rickert, C.; Koert, U. *Angew. Chem., Int. Ed.* **2000**, *39*, 900−902. (k) Murillo, O.; Suzuki, I.; Abel, E.; Murray, C. L.; Meadows, E. S.; Jin, T.; Gokel, G. W. *J. Am. Chem. Soc.* **1997**, *119*, 5540−5549. (l) Gokel, G. W. *Chem. Commun.* **2000**, 1−9. (m) Tedesco, M. M.; Ghebremariam, B.; Sakai, N.; Matile, S. *Angew. Chem., Int. Ed. Engl.* **1999**, *38*, 540−543. (n) Baumeister, B.; Sakai, N.; Matile, S. *Angew. Chem., Int. Ed.* **2000**, *39*, 1955−1958. (o) Merritt, M.; Lanier, M.; Deng, G.; Regen, S. L. *J. Am. Chem. Soc.* **1998**, *120*, 8494−8501. (p) Janout, V.; Giorgio, C. D.; Regen, S. L. *J. Am. Chem. Soc.* **2000**, *122*, 2671−2672. (q) Otto, S.; Osifchin, M.; Regen, S. L. *J. Am. Chem. Soc.* **1999**, *121*, 10440−10441. (r) Renkes, T.; Schäfer, H. J.; Siemens, P. M.; Neumann, E. *Angew. Chem., Int. Ed.* **2000**, *39*, 2512−2516. (s) Fritz, M. G.; Walde, P.; Seebach, D. *Macromolecules* **1999**, *32*, 574−580. (t) Qi, Z.; Sokabe, M.; Donowaki, K.; Ishida, H. *Biophys. J.* **1999**, *76*, 631−641. (u) Voyer, N.; Potvin, L.; Rousseau, E. *J. Chem. Soc., Perkin Trans. 2* **1997**, 1469−1472.

(6) Kobuke, Y.; Nagatani, T. *Chem. Lett.* **2000**, 298−299.

Scheme 1

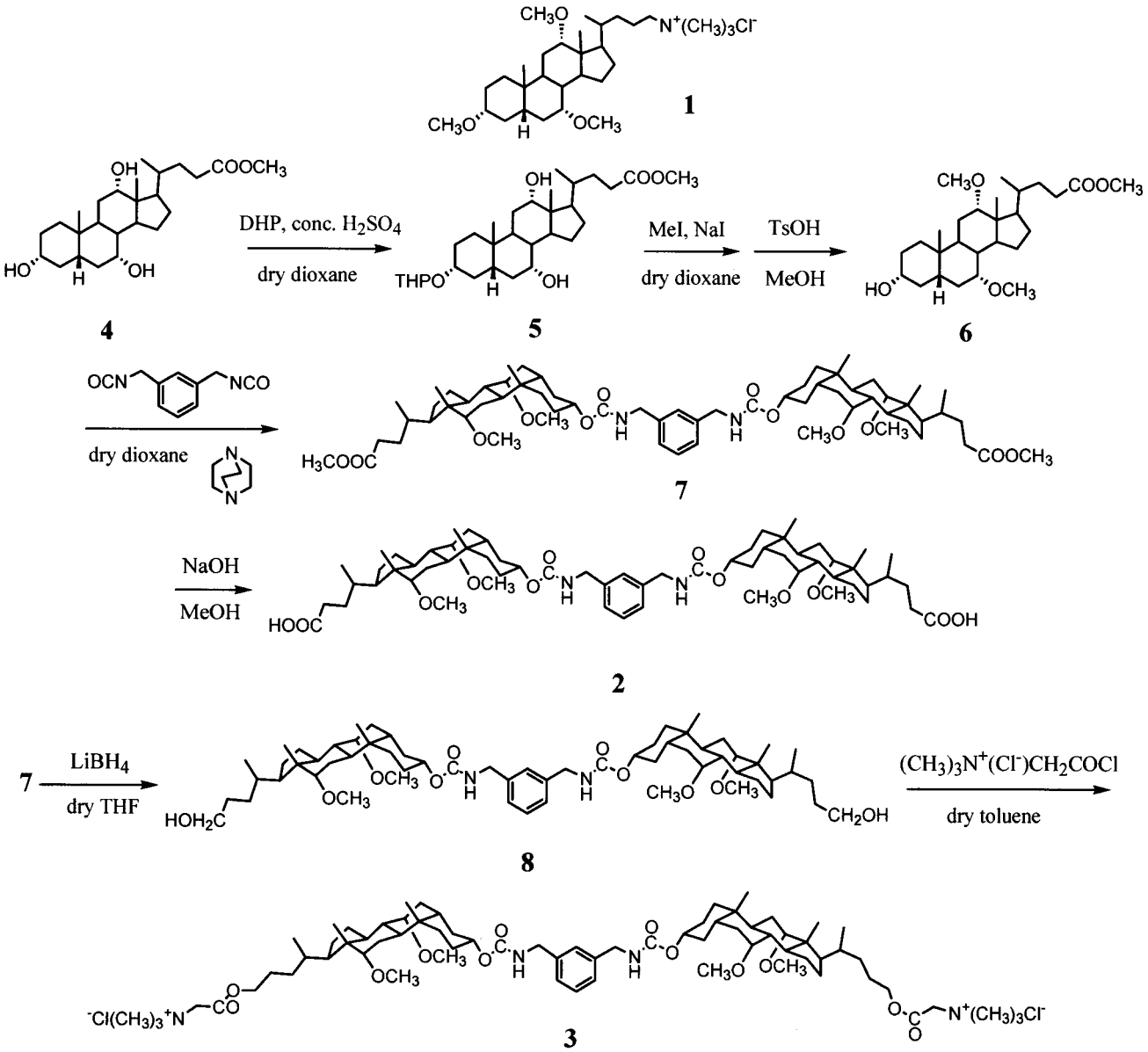

From these data, permeability selectivity ratios between Br^- and Cl^- anions are calculated as follows:

$$\mathbf{2}:\ P_{Br^-}/P_{Cl^-} = 3.0,\ \mathbf{3}:\ P_{Br^-}/P_{Cl^-} = 1.8$$

Metal Ion Selectivity. The permeability selectivity ratio between K^+ and Na^+, P_{K^+}/P_{Na^+} was obtained with application of a salt concentration gradient across the membrane by employing 500 mM each of KCl and NaCl at pH 7.2 (Figure 3). The reversal potentials here evaluated and the charge selectivity ratio P_{K^+}/P_{Cl^-} obtained above afforded almost the same permeability ratios P_{K^+}/P_{Na^+} upon 3.1 and 3.2 for **2** and **3**, respectively. The difference in the sign of terminal ionic groups did not significantly affect the metal ion selectivity.

To observe possible Li^+ currents, detection of single-channel currents was attempted using salt concentrations of 500 mM for both KCl and LiCl for the cis and trans sides, respectively, at pH 7.2. The channel component employed was **2**, and channel currents were traced for a total observation time of 1310 min with repeated exchange of bilayer lipid membrane as well as renewed incorporation of premixed channel solutions. During all these trials, currents were observed only for the period when applying positive voltages. Since the trans side is grounded, the observed currents always reflect the direction from the cis to trans sides, i.e., K^+ currents. We therefore conclude that no Li^+ currents can be generated. The observed $I-V$ plot shown in Figure 4 suggested the presence of two conductance levels of K^+ flux.

Discussion

Conductance. In the case of the half-channel stage, a trimethyl ether derivative of cholic acid itself could not afford ionic currents across the planar bilayer membranes. Successful ionic currents were observed only after conversion of the carboxyl terminal to a trimethylammoniomethyl grouping.[6] In the case when the membrane-penetrating unit was employed, both **2** and **3** were active in giving ionic currents. The channel structure seems to have been stabilized greatly by the use of a transmembrane component. The conductance levels varied in the range 5−20 pS for both of ion channels obtained from **2**

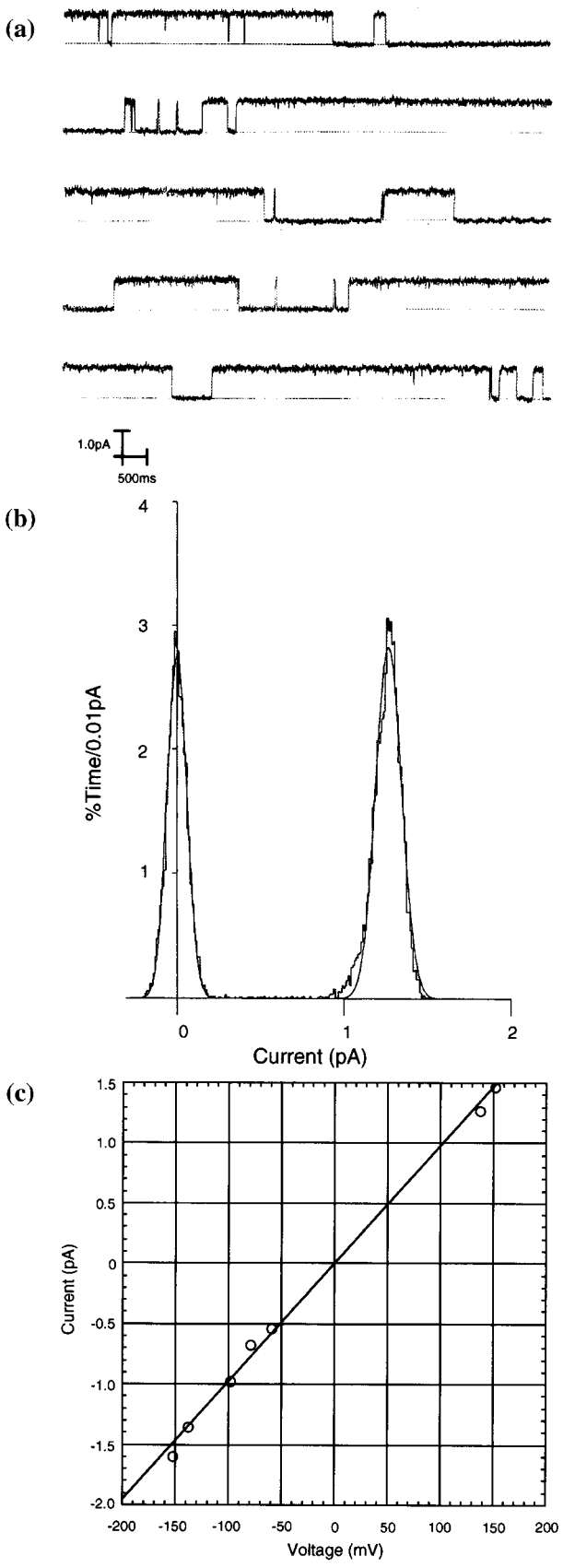

Figure 1. Typical example of basic behavior of transmembrane channel **2** at +73 mV under symmetric 500 mM KCl solutions at pH 7.2: (a) typical single-channel currents; (b) amplitude histogram of single-channel currents; (c) current−voltage relationship. Open squares and open circles stand for different runs. The estimated single-channel conductance from the slope was 17.3 pS for this run.

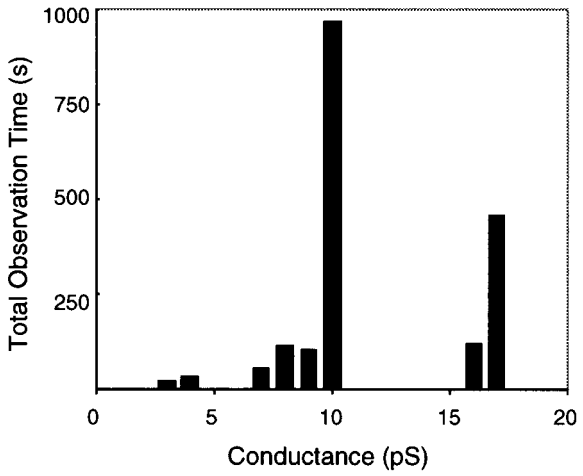

Figure 2. Histogram analysis of conductances observed for **2** for total observation time of 1840 s.

and **3**. Among these values, the most frequently observed conductances were 10 and 17 pS for **2** and 9 pS for **3** according to the histogram analysis of the total record time of 1840 s. The presence of different conductance levels is a characteristic of supramolecular ion channels,[5b] since the assembly number is determined by competition between the pore-making tendency by assembling amphiphilic molecules in the hydrophobic lipid components and the pore-suppressing power of lipids to maintain the defect-free assembly structure as their primary function. The process is an equilibrium and the structure is determined by several factors, including the nature of the lipid and amphiphile and amphiphile concentration. Several structures with different assembly numbers usually exist in membranes, and each measurement observes one of these. It is worth mentioning that the conductance range is similar to the value observed for naturally occurring Na^+ and K^+ ion channels. The range observed for Na^+ and K^+ channels fell within fairly narrow limits of 12.0 ± 5.2, 18.6 ± 14.6, 17.9 ± 11.3, 17.3 ± 13.7, for Na^+ channels, delayed rectifier K^+ channels, inward rectifiers, and transient A-type channels, respectively.[7] The results may be rationalized by the fact that these channels are constructed with very slight structural in order to recognize the subtle differences of Na^+, K^+, and other ionic species. In accord with this principle, conductances of acetylcholin receptor channels, nonselective toward a series of alkalimetal ions, are distributed in relatively large area 37.9 ± 8.0 pS. Investigation of charge and metal ion selectivities of channels obtained here is therefore interesting because similar conductance levels are expected to be associated with similarities in the pore size and the conducting pathway. These conductances fall in the range also observed for the supramolecular channels constructed from cholic acid methyl ether derivatives reported recently,[6] but are different from those of supramolecular channels obtained from oligo(butyleneoxy) chain units in view of their magnitude distribution, values varying in the range 10^1−10^3 pS.[2] Small conductances with a narrow distribution range for cases with steroidal units indicate that only limited numbers of the channel components are assembled to form the supramolecular channel.

(7) Data were taken from Figure 7, p 333 in ref 1 and analyzed.

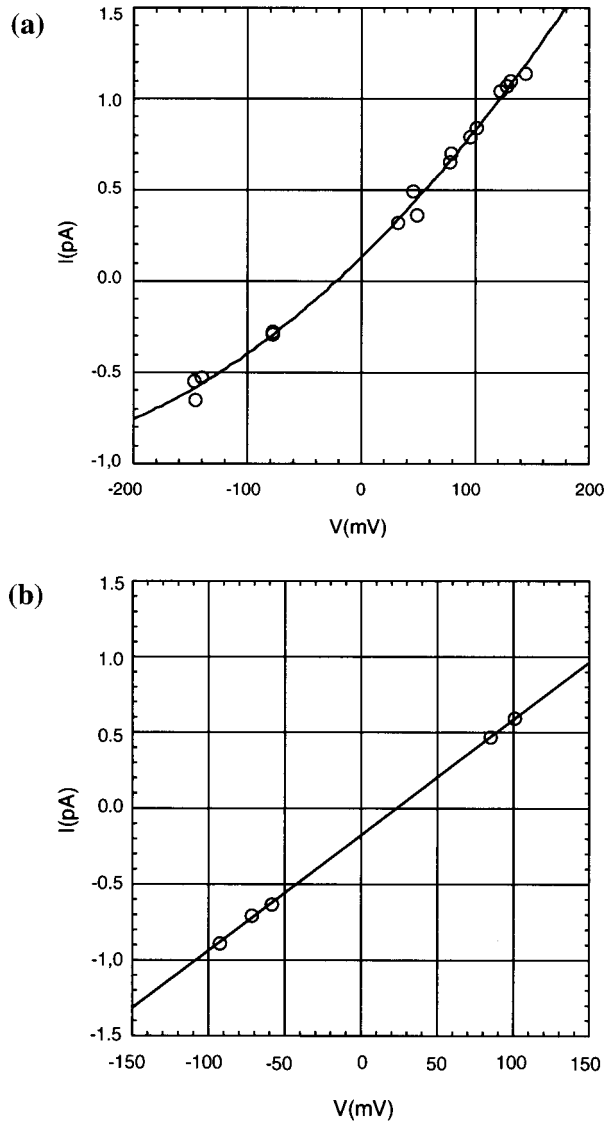

Figure 3. Current−voltage relationships under asymmetric salt concentrations: (a) $[KCl]_{cis} = 500$ mM, $[NaCl]_{trans} = 500$ mM for **2**; (b) $[NaCl]_{cis} = 500$ mM, $[KCl]_{trans} = 500$ mM for **3**.

Open-Closed Transitions. Single-channel recordings revealed characteristically long-lasting open states. Once a channel was opened, it remained so for at least 10 ms, mostly in the range of 10^2 ms to 10^1 s and even as long as 10 s in some cases. Typical histogram analyses for **2** are illustrated in Figure 3a,b of the Supporting Information. These data showed the existence of two apparently different open lifetimes of 125 and 3500 ms, respectively. Similar analyses for the data for **3** gave 800 and 5000 ms as typical open lifetimes. The existence of such extremely long lifetimes unfortunately limited the number of data points. Twenty-seven data points being obtained for longer lifetime events compared to 458 for the shorter ones, for **2** and 58 and 327 data points, respectively, for **3**. Even within these limitations, especially in view of the rather semiquantitative values for the longer lifetime events, the extremely stable nature of the open state of these transmembrane channels and the coexistence of at least two open lifetimes has clearly been demonstated. The tendency to exhibit long lifetimes has already been observed when supramolecular ion

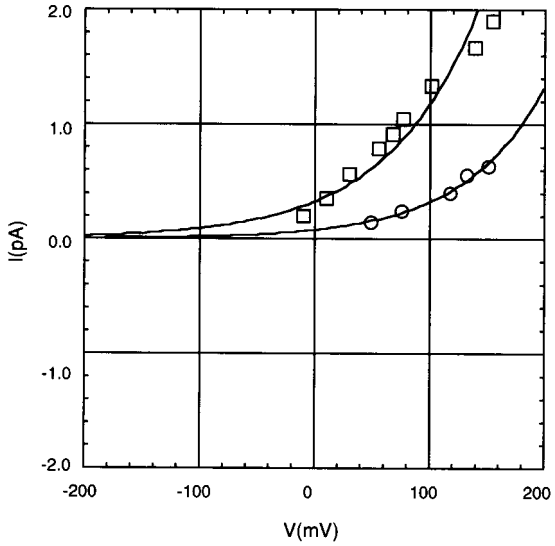

Figure 4. Current−voltage relationships for **2** under asymmetric salt concentrations, $[KCl]_{cis} = 500$ mM, $[LiCl]_{trans} = 500$ mM. The trans chamber is grounded. Open squares and open circles stand for different runs.

channel were constructed from cholic acid methyl ether derivatives as a half channel unit.[6]

This open lifetime may be compared to the value for gramicidin, 0.56 ± 0.06 s measured in soybean lecithin membranes.[8] Gramicidin is believed to exist as a rigid β-sheet structure stabilized by a hydrogen-bonded network in a conformationally immobile form. The open-closed transitions are ascribed to the encounter-separation kinetics of the two-half-channel components existing in different lipid layers. The open−closed transition, observed here for channels composed of membrane-spanning units occurs through association−dissociation processes of components oriented vertically to the membrane surface. This mechanism differs from the gramicidin case. However, the existence of similar and even longer open lifetimes certainly originates not only from the rigid steroidal skeletons but also from the stable polar interactions of methoxy groups forced to be assembled in surrounding nonpolar lipids.

Compared to these cases, short-lived on−off transitions were observed for ion channels having alkyl chains as the membrane-insertible component, such as ion pair channels composed of the oligoethercarboxylate−dialkylammonium,[2] oligoetherphosphate−dialkylammonium pair,[3a] or oligoetherammonium−alkyl phosphate ion pair,[3b] and alkylresorcin[4]arene.[4] The short-lived transitions in these cases could therefore be ascribed to fast molecular fluctuation of flexible alkyl chains in the membrane.

Charge Selectivity. Both of ion channels from **2** and **3** showed relatively high cation permeability selectivity ratios, P_{K^+}/P_{Cl^-} being 17 for **2** and 7.9 for **3**. This trend of cation selectivity exhibits similarities not only to channels linked by amphiphilic steroidal half-channel units, but also to many other artificial ion channels.[5b] In the present case, methoxy substituents are extruded from a rigid and hydrophobic steroidal skeleton and placed with appropriate separation distances in lipid membranes. These polar substituents are thought to be arranged favorably to incorporate metal ions into membranes and transport

(8) Russel, E. W.; Weiss, L. B.; Navetta, F. I.; Koeppe, R. E., II; Andersen, O. S. *Biophys. J.* **1986**, *49*, 673−686.

Table 1. Conductances and Permeability Selectivity of Artificial and Natural Ion Channels

channel	conductance (pS)	permeability ratio P_{K^+}/P_{Cl^-}	permeability ratio P_{K^+}/P_{Na^+}	ref
acetylcholine receptor	28	large[a]	1.1	9
gramicidin A	~17	large[a]	3.5	10
10	2−10	6.1	6.1	3c
2	5−20 (10, 17)[b]	17	3.1	this work
3	5−10 (9)[b]	7.9	3.2	this work
oligoether ion pair	100−1000	5	nonselective	2
calix[4]arene	6.1	20	3	4
THF−gramicidin	15.4, 19.7	ND[c]	2.7	5d
AC164	9	23	2.5	5t
$Ac(LSSLLSL)_3$	21	10	*1.2*[d]	11
macro-D,L-peptide	65	ND	*1.2*[d]	12

[a] No measurable anionic currents are reported. [b] Values in parentheses show main components. [c] ND: not determined. [d] Italic values report conductance ratios.

them by successive coordination of lone pairs to metal ions, which are otherwise stabilized by being fully solvated in the aqueous phase. Such an arrangement may contribute negatively to incorporation and transport of halide anions giving rise to preferences toward transport of cations over anions.

Comparison of absolute values of the charge selectivity ratio indicates the effect of external charges on charge selectivity. The difference in cation selectivity values between channels obtained from **2** and **3** may reasonably be accounted for by the different charges located at the surface of the channel. Positively charged ammonium in **3** may accumulate anions in the area at the entrance of the channel and contribute to a decrease in the cation/anion selectivity ratio. In turn, the carboxylate anion in **2**, may increase metal cation concentrations at the surface to effect an increase in the selectivity ratio. A similar modulation of cation selectivity has also been reported for peptide bundle channels.[5f] Insertion of a glutamate or arginine residue near the N-terminus of a neutral Ac-$(LSSLLSL)_3$ peptide bundle increased the selectivity to infinity or decreased it to be almost nonselective, respectively, compared to the moderate original value at $P_{K^+}/P_{Cl^-} = 10$.

Metal Ion Selectivity. The transmembrane ion channel bearing carboxylate headgroups **2** showed metal ion selectivities in the decreasing order of $K^+ > Na^+ \gg Li^+$, no Li^+ currents being observed. Although the detection of possible Li^+ currents for **3** having ammonium headgroups was not attempted, two ion channels obtained from **2** and **3** gave similar permeability selectivity ratios P_{K^+}/P_{Na^+} of 3.1 and 3.2, respectively. The similar selectivity ratios of channels obtained from **2** and **3** having oppositely charged headgroups is suggestive that the metal ion selectivity is determined primarily at the critical domain of the lipid membrane located in the interior and separated substantially from the ionic headgroups.

Even though the artificial ion channels constructed here were composed of several amphiphilic molecular units and provide different conductance levels rather than any specific level, the channels can differentiate K^+ from Na^+ ions and from Li^+ ion with a much higher differentiation factor. It is interesting to note that reversal potentials, i.e., metal ion selectivities fall into the same value for channels having different conductance values. Moreover, the metal ion selectivities observed here are some of the highest among the various approaches used to create artificial ion channels, as judged from the selectivity data listed in Table 1. Metal ion selectivities are reported for artificial and natural ion channels, along with the conductance and charge selectivity data. There is a tendency that significant K^+/Na^+ selectivities are observed when conductances are relatively small, i.e., less than about 20 pS. This may be most obvious if one compares the oligoether azo channel **10**[3c] and oligoether ion pair channels.[2] The former with small conductances gave significant K^+/Na^+ selectivity. Compared to this, oligoether ion pair channels[2] with a similar ether moiety lost K^+/Na^+ selectivity completely, when the selectivity was examined under high conductance states. Peptide bundles $Ac(LSSLLSL)_3$[11] and stacked macro-D,L-peptides[12] with larger conductances gave only marginal conductance ratios.

In order for metal ions to be transported across the hydrophobic membrane barriers, they must be desolvated to some extent and the selectivity may thus be correlated to the relative ease of dehydration as a first approximation. The observed selectivity data matched well with the relative order of hydration energies: K^+ (85 kcal/mol) < Na^+ (105 kcal/mol) ≪ Li^+ (131 kcal/mol). For a smaller hydration energy, the metal ion is more easily desolvated and stabilized in the membrane phase even by weak stabilizing interactions. Ionic species having larger hydration energies are difficult to desolvate completely, difficult to incorporate into the membrane phase and difficult to be transported. The crystal structure of the KcsA K^+ channel from *Streptomyces lividans*[13] has made clear the stabilizing coordination toward K^+ ion near the selectivity filter constructed only from neutral peptide carbonyls. The favorable selectivity toward K^+ over Na^+ may indicate that the channel provides only a weakly stabilizing environment toward the metal ions to be transported. For potential ion channels exhibiting reverse selectivity, i.e., favoring Na^+ over K^+, it may be necessary to introduce a stronger electric field to stabilize the Na^+ ion, as suggested for the selectivity filter of voltage-gated Na^+ channels.[14] The lack of observable Li^+ currents may reasonably be accounted for by the ion's very high

(9) Adams, D. J.; Dwayer, T. M.; Hill, B. *J. Gen. Physiol.* **1980**, *75*, 493−510.
(10) Myers, V. B.; Haydon, D. A. *Biochim. Biophys. Acta* **1972**, *274*, 313−322.
(11) Lear, J. D.; Wasserman, Z. R.; DeGrado, W. F. *Science* **1988**, *240*, 1177−1181.
(12) Ghadiri, M. R., Granja, J. R.; Buehler, L. K. *Nature* **1994**, *369*, 301−304.
(13) Doyle, D. A.; Cabral, J. M.; Pfuetzner, R. A.; Kuo, A.; Gulbis, J. M.; Cohen, S. L.; Chait, B. T.; Mackinnon, R. *Science* **1998**, *280*, 69−77.
(14) (a) Hille, B. *Fed. Proc.* **1975**, *34*, 1318−1321. (b) Hille, B. *J. Gen. Phys.* **1975**, *66*, 535−560.

hydration energy. A similar sharp discrimination factor between Na^+ and Li^+ ions was reported only from Sokabe et al.[5t] for artificial single-ion channels when using the hydrophobic ion channel AC164, where a macrocyclic octapeptide was attached with long alkyl chains.

The anion permeability selectivity ratio for P_{Br^-}/P_{Cl^-} has also been obtained. Again, favorable permeation was observed for the larger Br^- anion compared to the smaller Cl^-. The small discrimination factor is compatible with the small difference in solvation energies between Br^- and Cl^-, being 79 and 82 kcal/mol, respectively.

Conclusion

In conclusion, we have obtained a new class of supramolecular transmembrane ion channels using construction units having molecular amphiphilicity. A bisurethane-linked bis(7,12-dimethoxycholanyl) moiety was used as the membrane-insertible unit and a carboxylate or ammonium external headgroup was used for **2** and **3**, respectively. The units gave rise to the formation of stable ion channels characterized by relatively small conductances and long lasting open states. High cation/anion selectivities were demonstrated and could be modulated by changing the ionic nature of the headgroup of channels. Both channels obtained from **2** and **3** exhibited metal ion selectivities discriminating K^+ from Na^+ by similar factors of 3.1−3.2, seemingly almost independent of the different external charges of the headgroup. No Li^+ current was observable, and the permeability selectivities between different alkali metals and halides seem to be determined primarily by desolvation energies of the ionic species.

Experimental Section

General Procedure. ^{1}H NMR spectra were recorded for $CDCl_3$ or DMSO-d_6 solutions on a JEOL EX270 spectrometer with tetramethylsilane ($\delta = 0$ ppm) as an internal standard. TOF-mass spectra were measured on a Perceptive Voyager RP through laser ionization with dithranol, DBH, or α-CHCA as matrixes or a Perceptive Mariner by electron spray ionization. IR spectra were recorded on a Hitachi 260-50 instrument or a Perkin-Elmer FTIR Spectrum2000. Soybean lecithin (type-IIS) was purchased from Sigma Chemical Co. Ltd. and used without purification. Solvents and chemicals were used as received unless otherwise noted. Thin-layer chromatography (TLC) was undertaken on a glass plate precoated with silica gel (E. Merck Kieselgel 60 F254) by visualizing the spots with UV light (254 nm) irradiation and/or iodine coloration. Column chromatography was performed with silica gel 60 (E. Merck, particle size 0.063−0.200 mm, 60−230 mesh).

Methyl 3a-(2′-Tetrahydropyranyl)cholate (5). Freshly distilled 2,3-dihydropyrane (1.22 g, 14.5 mmol) was added to a solution of methyl cholate (5 g, 14 mmol) dissolved in 50 mL of dry dioxane at room temperature. One or two drops of concentrated H_2SO_4 were added to the solution while it was cooling in an ice−water bath. The reaction was monitored by TLC at intervals of 5−10 min. After no significant change was observable, the reaction mixture was warmed to room temperature and neutralized with saturated aqueous sodium bicarbonate. The solvent was removed under reduced pressure, and the residue was extracted with $CHCl_3$ and subjected to a chromatographic separation (silica gel, benzene/AcOEt = 1:1, $R_f = 0.4$) to isolate 3-THP-protected methyl cholate **5** (3.15 g, 43%): ^{1}H NMR (270 MHz, $CDCl_3$) δ 3.82 (m, CHO, 1.2H(1H)), 3.95 (m, CHO, 1.0H(1H)), 3.90 (m, THP-OCH, 1.0H(1H)), 3.65 (s, CO_2CH_3, 3.0H(3H)), 3.45 (m, OCH_2(THP), 2.1H(2H)), 4.72 (m, OCHO(THP), 1.0H (1H)), 0.6−2.4 (other steroidal CH and CH_2, 44H (44H)).

Methyl 7,12-Dimethylcholate (6). NaH (60% in mineral oil, 750 mg, 19 mmol) was added to a solution of **5** (2.0 g, 4 mmol) in 50 mL of dry dioxane, and the mixture was refluxed for 1 h. After MeI (2.3 g, 16 mmol) was added at room temperature, refluxing was started again. While the reaction was monitored by TLC (benzene/AcOEt = 1:1), NaH (3 g, 75 mmol), and MeI (23 g, 160 mmol) were added in several portions over a period of 46 h, when the component at $R_f = 0.75$ did not increase any more. The solution was neutralized with 1 N HCl, concentrated, and extracted with ether. After removal of the solvent under reduced pressure, the residue was dissolved in 100 mL of MeOH, and $TsOH\cdot H_2O$ (20 mg) was added to cleave off the THP protecting group. The solution was stirred at room temperature until the spot at $R_f = 0.75$ was replaced almost completely by a new spot at $R_f = 0.4$. The solution was neutralized with sodium bicarbonate. After filtration, the reaction mixture was concentrated and subjected to column chromatography (benzene/AcOEt = 1:1) in order to isolate the fraction at $R_f = 0.4$: yield 400 mg, 16%; ^{1}H NMR (270 MHz, $CDCl_3$) δ 3.20 (m, $-OCH_3$, 3.2H (3H)), 3.26 (m, $-OCH_3$, 3.0H(3H)), 3.41 (m, CHO, 1.1H(1H)), 3.15 (m, CH-hydroxyl, 1.1H(1H)), 3.36 (m, CHOC, 1.0H(1H)), 3.66 (s, CO_2CH_3, 3.0H(3H)), 0.6−2.4 (other steroidal CH and CH_2, 39.8H-(34H)).

Bis[(methyl 7,12-dimethyl-24-carboxylate)-3-cholanyl]-*N,N′*-xylylene Dicarbamate (7). Xylylene diisocyanate (91 mg, 0.49 mmol) and diazobicyclo[2.2.2]octane (DABCO, 12 mg, 0.097 mmol) were added to a solution of **6** (439 mg, 0.97 mmol) dissolved in 10 mL of dry dioxane at room temperature. The solution was heated at 70 °C for 7 h, and the solvent was evaporated under reduced pressure. Aqueous 1 N HCl solution was then added, and DABCO was removed by decantation. The supernatant was concentrated to dryness and applied for column chromatography (benzene/AcOEt = 4:1): yield 240 mg, 45%; ^{1}H NMR (270 MHz, $CDCl_3$) δ 3.20 (m, $-OCH_3$, 2.8H (3H)), 3.25 (m, $-OCH_3$, 3.0H (3H)), 4.47 (m, CHOCO, 1.0H (1H)), 3.15 (m, CHOC, 1.0H (1H)), 3.37 (m, CHOC, 1.0H (1H)), 3.65 (s, CO_2CH_3, 2.8H (3H)), 4.32 (m, Bz-CH_2, 1.8H (2H)), 4.90 (m, NH, 0.8H (1H)), 0.6−2.4 (other alkyl CH, 34.0H (34H)); MALDI-TOF (positive mode, DHB) *m/z* calcd for $C_{64}H_{100}N_2O_{12}$ 1088.73, found 1111.21 $(M + Na)^+$ and 1126.08 $(M + K)^+$.

Bis(7,12-dimethyl-24-carboxy-3-cholanyl)-*N,N′*-xylylene Dicarbamate (2). An aqueous solution of 3 mL of 1 N NaOH was added to a hot MeOH solution (60∼70 °C, 12 mL) of **7** (20 mg, 0.018 mmol), and the solution was stirred for 2 h. The solution was acidified with 1 N HCl (pH 4), and the solvent was removed under reduced pressure. The residue was extracted with $CHCl_3$, and the solution was concentrated to dryness under reduced pressure: yield 17 mg, 87%; ^{1}H NMR (270 MHz, $CDCl_3$) δ 3.20 ((m, $-OCH_3$, 3.0H (3H)), 3.25 (m, $-OCH_3$, 3.1H (3H)), 4.47 (m, CHOCO, 1.0H (1H)), 3.18 (m, CHOC, 1.2H (1H)), 3.39 (m, CHOC, 1.2H (1H)), 4.38 (m, Bz-CH_2, 2.0H (2H)), 4.98 (m, NH, 0.8H (1H)); MALDI-TOF (positive mode, dithranol) *m/z* calcd for $C_{62}H_{96}N_2O_{12}$ 1060.70, found 1083.94 $(M + Na)^+$ and 1099.98 $(M + K)^+$. Anal. Calcd for $C_{62}H_{96}N_2O_{12}$: C 70.16; H 9.12. Found: C 69.87, H 9.14.

Bis(7,12-dimethyl-24-hydroxy-3-cholanyl)-*N,N′*-xylylene Dicarbamate (8). A dry THF solution (1 mL) of $LiBH_4$ (2.0 mg, 0.09 mmol) was added dropwise with stirring to a solution of **7** (50 mg, 0.046 mmol) in 5 mL of dry THF, and the stirring was continued for 9 h at room temperature. The reaction mixture was poured into ice−water, and the pH was adjusted to weakly acidic, extracted with diethyl ether, and concentrated to dryness. The product **8** was purified by column chromatography (benzene/AcOEt = 4:1, $R_f = 0.4$): yield 18 mg, 38%; ^{1}H NMR (270 MHz, $CDCl_3$) δ 3.20 (m, $-OCH_3$, 3.0H (3H)), 3.25 (m, $-OCH_3$, 3.0H (3H)), 4.47 (m, CHOCO, 1.0H (1H)), 3.18 (m, CHOC, 1.0H (1H)), 3.39 (m, CHOC, 1.3H (1H)), 4.39 (m, Bz-CH_2, 2.0H (2H)), 4.95 (m, NH, 1.0H (1H)), 3.65 (t, CH_2O, 2.0H (2H)), 0.6−2.4, (other alkyl CH, 38.3H (36H)); MALDI-TOF (positive mode, α-CHCA) *m/z* calcd for $C_{62}H_{100}N_2O_{10}$ 1032.73, found 1055.73 $(M + Na)^+$ and 1071.71 $(M + K)^+$.

***N*-2-Chlorocarbonylmethyl-*N,N,N*-trimethylammonium Chloride (9).** Well-dried betain HCl salt (900 mg, 5.9

mmol) was added to thionyl chloride (1.2 mL, 16 mmol) and heated to 75 °C. After gas evolution ceased, a viscous yellow solution was obtained. Hot toluene (80 °C, 5 mL) was added, the solution was stirred well, and the upper toluene phase was decanted. To remove thionyl chloride, this procedure was repeated six times, and the final toluene suspension was used for the next reaction.

Bis[7,12-dimethyl-24-(*N*,*N*,*N*-trimethylethanaminium-2-carboxylate)-3-cholanyl]-*N*,*N*′-xylylene Dicarbamate Dichloride (3). A toluene suspension (5 mL) of **9** (5.9 mmol) and pyridine (476 μL, 5.9 mmol) were added with stirring to a solution of **8** (40 mg, 3.9 mmol) in toluene (5 mL). The solution was stirred for 18 h at room temperature. Solvents were removed under reduced pressure, and the residue was subjected to column chromatography ($CHCl_3$/MeOH/H_2O = 30:12:5, R_f = 0.35) to give 3 mg, 2%: ^{1}H NMR (270 MHz, $CDCl_3$) δ 3.19 (m, $-OCH_3$, 3.0H (3H)), 3.27 (m, $-OCH_3$, 3.0H (3H)), 4.49 (m, CHOCO, 1.0H (1H)), 3.15 (m, CHOC, 1.0H (1H)), 3.39 (m, CHOC, 1.0H (1H)), 4.32 (m, Bz-CH_2, 2.0H (2H)), 5.00 (m, NH, 1.0H (1H)), 3.65 (s, $N^+(CH_3)_3$, 9.3H (9H)), 4.18 (s, CH_2-OCO, 1.7H (2H), 5.10 ($COCH_2$, 1.7H (2H)), 0.6−2.4, (other alkyl CH, 47.7H (36H)); ESI-TOF (positive mode, α-dithranol) *m*/*z* calcd for $\mathbf{3}^{2+}$ $C_{72}H_{120}N_4O_{12}$ 616.445, found 616.3. Anal. Calcd for $C_{72}H_{120}N_4O_{12}Cl_2 \cdot 2H_2O$: C, 64.50; H, 9.32. Found: C, 64.32; H, 9.31.

Measurement of Single-Channel Currents. Single-channel currents were observed by using a planar bilayer system. The artificial ion channel compound **2** or **3** was premixed with soybean lecithin in decane (40 mg/mL). Bilayers were formed by applying the mixed solution to a hole of 0.2−0.3 mm in diameter, precoated with a more concentrated lecithin solution in decane (80 mg/mL), and dried prior to the measurement. The concentrations of channel forming compounds **2** and **3** were mostly 1 wt % relative to lecithin, but were also investigated in the range 0.1−5 wt %. The concentrations of **2** or **3** were varied, and no appreciable difference was observed in the single-channel behaviors.

The currents across the bilayer were low-pass filtered at 0.40 kHz, fed into a patch-clamp amplifier (CEZ-2300, Nihon Kohden) and recorded on a magnetic tape through a PCM recorder (VR-10B, Instrutech Corp.). One of the chambers was connected to the signal ground of the amplifier and was defined as the trans side. The voltage was referred to the opposite cis side with respect to the trans side. All solutions used were buffered by 5 mM HEPES and adjusted with Tris base to pH 7.2. All experiments were carried out at room temperature (20−25 °C).

Charge and metal ion selectivities were obtained as permeability selectivity ratios P_{K^+}/P_{X^-}, P_{K^+}/P_{Na^+} by introducing reversal potentials Erev's from current−voltage (I−V) plots under asymmetric ionic conditions into the Goldman−Hodgkin−Katz equations GHK-1 and GHK-2, respectively.

$$E_{rev} = (RT/F)\ln(P_{K^+}[K^+]_t + P_{X^-}[X^-]_t)/(P_{K^+}[K^+]_c + P_{X^-}[X^-]_c) \qquad \text{GHK-1}$$

$$E_{rev} = (RT/F)\ln(P_{K^+}[K^+]_c + P_{Na^+}[Na^+]_c + P_{Cl^-}[Cl^-]_t)/(P_{K^+}[K^+]_t + P_{Na^+}[Na^+]_t + P_{Cl^-}[Cl^-]_c) \qquad \text{GHK-2}$$

where $[M^+]$ and $[X^-]$ represent the activities of ions M^+ and X^-, subscripts c and t represent the cis and trans sides of the chamber, and the other parameters have their conventional meanings. The activity coefficient of each ion was estimated from Debye−Hückel equations.

Data Analysis. Single-channel currents recorded on magnetic tape were replayed, post-filtered at 0.10 kHz, and digitized at 0.50 ms/points by means of A/D converter (model 2801A, Data Translation Co.). The amplitude of the single-channel currents was measured as a peak-to-peak distance (each peak represents open and closed levels) on the amplitude histogram by use of a single-channel analysis program, PAT (version 6.2) written by Dr. John Dempster (University of Strathclyde, Glasgow, U.K.). Single-channel conductance values were determined from the slope of current−voltage plots under symmetric salt solution conditions.

The deviation of offset potential was carefully checked before and after each run, especially for measurements under asymmetric ionic conditions. When any deviation from the initial zero-adjustment was observed after the run, the data set was eliminated from the record.

Acknowledgment. The authors are grateful for helpful discussion by Prof. Masahiro Sokabe at Graduate School of Medicine, Nagoya University.

Supporting Information Available: Current−voltage relationships under asymmetric salt concentrations for **2** and **3** are given in Figures 1 and 2, respectively. Histogram analysis of open lifetime of **2** are given in Figure 3. This material is available free of charge via the Internet at http://pubs.acs.org. This material is contained in libraries on microfiche, immediately follows this article in the microfilm version of the journal, and can be ordered from the ACS; see any current masthead page for ordering information.

JO010208I